Study on Seismic Performance Upgrading for Steel Bridge Structures by Introducing Energy-Dissipation Members

Zhiyi Chen*, Hanbin Ge**, and Tsutomu Usami ***

* Graduate Student, Dept. of Civil Eng., Nagoya University, Furo-cho, Chikusa-ku, Nagoya 464-8603
** Dr. Eng., Associate Professor, Dept. of Civil Eng., Nagoya University, Furo-cho, Chikusa-ku, Nagoya 464-8603
*** Dr. Sc., Professor, Dept. of Civil Eng., Meijo University, 1-501 Shiogamaguchi, Tenpaku-ku, Nagoya 468-8502

The seismic performance upgrading effects for steel bridge structures by introducing energy-dissipation members are investigated in this paper. The energy-dissipation members concerned in the present study are shear panel dampers and buckling-restrained braces, which dissipate seismic energy through metallic yielding. This investigation is divided into two parts: (1) an introduction of design details and modeling for energy-dissipation members; (2) a parametric study on seismic responses of various frame-type bridge piers with energy-dissipation members. Three parameters, the strength ratio, stiffness ratio, and displacement ratio, are identified as design criteria to investigate the performance of bridge structures with the energy-dissipation members. Significant seismic performance upgrading effects have been found numerically. The results show that the parameters can be used as key parameters in unified design of such energy-dissipation members.

Key Words: seismic performance upgrading, steel bridge, energy-dissipation member

1. Introduction

In recent years, various structural control technologies have been developed and used successfully into building structures to suppress structural vibrations induced by earthquakes. Of these technologies, the use of energy-dissipation members proves to be a promising way to alleviate seismic response of structures. The energy-dissipation members concerned in the present study are shear panel dampers (SPD) and buckling-restrained braces (BRB), which dissipate seismic energy through metallic yielding and therefore add supplemental structural damping. The examples of single-deck bridge piers installed with SPD and BRB are shown in Fig. 1. Methods of increasing damping through metallic yielding have been validated to be effective. Use of energy-dissipation members has additional advantages of absorbing the bulk of seismic energy input and suffering major damage so as to keep the main structural members in an elastic state or only limited damage. After an earthquake these energy-dissipation members are ready to be replaced.

Detailing of some energy-dissipation members and their applications in building structures has been presented in numerous literatures[1)-3)], however the research on bridge structures remains infancy[4), 5)]. Distinguished from steel building structures, thin-walled steel bridge structures are usually made of steel plates with large width-thickness ratio, which are susceptive to local buckling. During the 1995 Hyogoken-Nanbu earthquake, a large amount of critical buckling has been observed at several critical member segments of the thin-walled steel bridge structures[6)]. Such damage occurs locally, but affects globally. Therefore it is also interesting to investigate the seismic upgrading effects of energy-dissipation member on alleviating local damage of such bridge structures in addition to global structural performances as for building structures.

Energy-dissipation members within bridge structures are often designed against extremely severe earthquakes. Therefore it

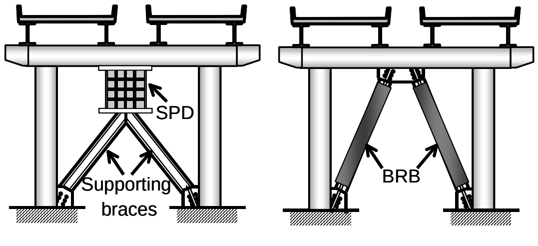

(a) SPD (b) BRB

Fig.1 Bridge piers with energy-dissipation members is better to use conventional mild steel as the yielding material rather than extremely low-yield steel to ensure sufficient energy dissipation. For this reason, SPD and BRB adopted in this study are made of conventional mild steel grade SS400. The hysteretic behavior of energy-dissipation members made of such steel grade is characterized by kinematic hardening rule according to the previous work[7), 8)]. Detailed design and modeling of SPD and BRB to be used in bridge structures will be addressed later.

The main purpose of this study is to identify the seismic upgrading effects of SPD and BRB and, furthermore, to present unifying criteria for design of energy-dissipation members of this kind in different bridge structure forms. For these purposes, the concepts and key design parameters are presented first, which form the basis of subsequent design to compare seismic responses of two types of energy-dissipation members quantitatively. Followed are introduction of restoring models of BRB and SPD as well as their analytical modeling, preparing for dynamic time-history analysis. This investigation may provide useful messages for practical design so as to improve the wider spread acceptance for energy-dissipation members in bridge structures. Information and analytical modeling of sample bridge structures are presented subsequently, covering a wide range of structure types, such as single-deck bridge piers, multi-deck bridge piers and single-deck bridge piers with different frame shapes. An extensive parametric study is then carried out and seismic behavior of the bridge structures installed with energy-dissipation members is studied. Although considered here are simple bridge structures of frame type, the basic principles and findings can be extended to more complicated bridge structures.

2. Concepts and Design Criteria of Controlled Structures

In this paper, a main structure installed with energy-dissipation members is referred to as a controlled structure since its seismic behavior may be controlled by energy-dissipation members properly designed. Sketches of physical models for a controlled structure installed with SPD and BRB are shown in Figs. 2 and 3, respectively.

As is seen from Fig. 2(a), SPD and supporting braces are connected in series manner and compose an energy-dissipation device (Fig. 2(b)). Hereafter, the corresponding features about the shear panel damper, the supporting braces, the energy-dissipation device and the main structure will be denoted by the subscripts *SPD*, *SB*, *d*, and *f*, respectively. Note that the lateral yield strength of supporting braces should be larger than the shear strength of SPD ($F_{y,SB}>F_{y,SPD}$) as shown in skeleton curves of separate shear panel and supporting braces. In other words, the lateral yield resistance of the energy-dissipation device is equal to the shear strength of SPD ($F_{y,d}=F_{y,SPD}$). Then, the entire energy-dissipation device is incorporated into the main structure in the parallel manner. The superposition of the skeleton curves of the energy-dissipation device and the main structure gives a trilinear force-displacement relationship for the controlled structure (see Fig. 2(c)), where design conditions of $\delta_{y,d} < \delta_{y,f}$ and $\delta_{y,fd} = \delta_{y,d}$ must be satisfied.

Compared to the structure installed with SPD, the concept of a structure with BRB is relatively simple. Referring to Fig. 3, BRB member may be viewed as an entire energy-dissipation device for simplicity. Consequently, the basic properties of an energy-dissipation device have the same meaning as those of the BRB members (i.e., $F_{y,d}=F_{y,BRB}$, $K_d=K_{BRB}$). The BRB members are then connected as a whole with the main structure in the parallel manner. It is clear that the yield displacement of BRB must be smaller than that of the main structure to ensure BRB yields prior to the main structure during an earthquake. That is to say, the design conditions of $\delta_{y,d} < \delta_{y,f}$ and $\delta_{y,fd} = \delta_{y,d}$ are also required for structures installed with BRB.

According to the concepts of a controlled structure described above, the following three parameters are proposed as design

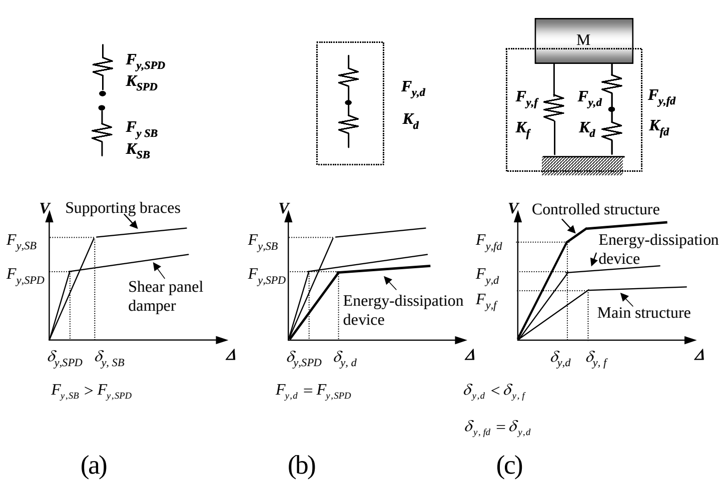

Fig.2 Idealized SDOF system installed with SPD

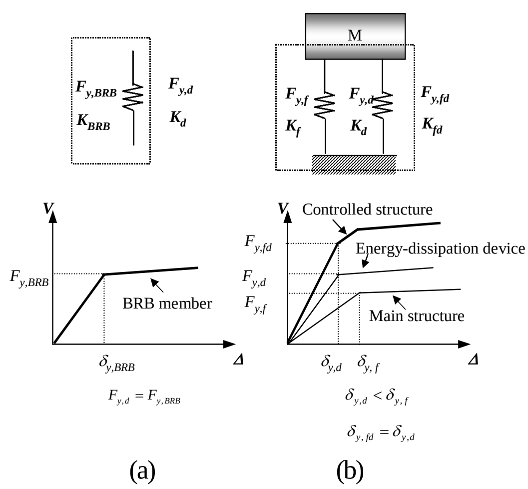

Fig.3 Idealized SDOF system installed with BRB

criteria to investigate seismic responses quantitatively:

(1) The strength ratio, α_F

$$\alpha_F = \frac{F_{y,d}}{F_{y,f}} = \frac{\text{Yield strength of energy-dissipation device}}{\text{Yield strength of main structure}}$$

(2) The stiffness ratio, α_K

$$\alpha_K = \frac{K_d}{K_f} = \frac{\text{Elastic stiffness of energy-dissipation device}}{\text{Elasitc stiffness of main structure}}$$

(3) The displacement ratio, α_δ

$$\alpha_\delta = \frac{\delta_{y,d}}{\delta_{y,f}} = \frac{\text{Yield displacement of energy-dissipation device}}{\text{Yield displacement of main structure}}$$

All three parameters take account of the direct relationship between a main structure and an energy-dissipation device. Past researches have shown that α_F, α_K, α_δ, and other similar parameters govern the performance of a controlled structure[9)-11)]. It has been pointed out that damage to the main structure can be minimized at a certain strength ratio α_F around an optimum strength ratio value, which depends on α_K[9)]. In another work[10)], it is argued that α_F has a primary influence on top displacement responses and ductility of structures while the stiffness ratio α_K shows less influence. An alternative parameter serving as a design criterion is equivalent viscous damping, which is based on the concept of equivalent energy[12)]. Here, α_F and α_K will be employed because they are more straightforward than the equivalent viscous damping parameter. The design criteria also adapt to the current design specifications, and consequently they are easily understood by engineers. In addition, it should be noted that two of the three parameters are independent for the SPD device, while all parameters are mutually dependent for the BRB device, as will be explained later. Therefore, α_F is taken as a solely adjustable parameter for design of the BRB device. For quantitative comparisons, the SPD device is then proportioned to have the same α_F and α_K of the BRB device.

3. Design and Modeling of Energy-Dissipation Devices

3.1 Shear panel damper (SPD) devices

(a) *Basic properties of shear panel damper*

The typical elevation of shear panel damper and its skeleton curve are shown in Fig. 4. Its basic properties are presented as follows:

$$F_{y,SPD} = \tau_y b_w t_w, \delta_{y,SPD} = \gamma_y a, K_{SPD} = b_w t_w G / a \quad (1a)$$

$$F_{u,SPD} = \tau_u b_w t_w, \ \delta_{u,SPD} = \gamma_u a \quad (1b)$$

where $F_{y,SPD}$ = yield strength, $\delta_{y,SPD}$ = yield displacement, $F_{u,SPD}$ = ultimate strength, $\delta_{u,SPD}$ = ultimate displacement, and K_{SPD} = initial elastic stiffness of a SPD. b_w, t_w, and a = geometrical

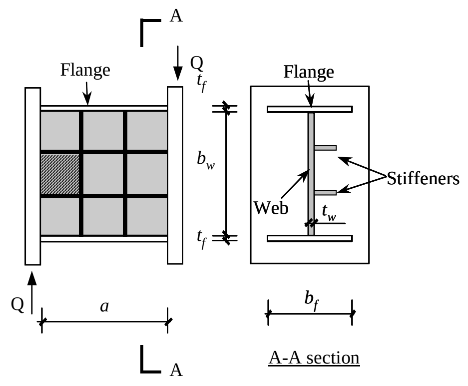

(a) Elevation

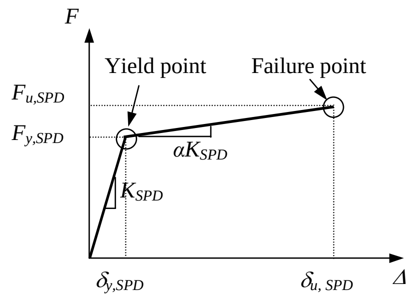

(b) Skeleton curve

Fig.4 Shear panel damper (SPD)

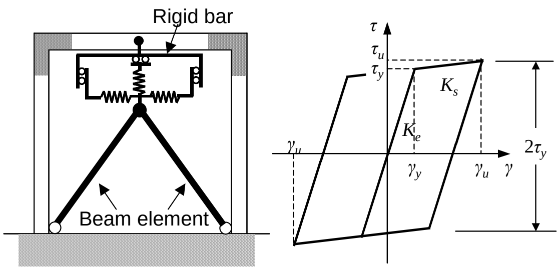

Fig.5 SPD model

parameters, see Fig. 4(a). τ_y and γ_y = shear yield stress and strain of web steel, τ_u and γ_u = ultimate shear strength and shear strain of SPD, which can be calculated from the formulas developed by Chen et al.[7)]

(b) *Basic properties of supporting braces*

It is assumed that supporting braces remain elastic during an earthquake. The consideration of the elastic relationship gives:

$$F_{y,SB} = \sigma_{y,SB} A_{SB} \frac{L}{l_{SB}}, \ K_{SB} = A_{SB} \frac{EL^2}{2 l_{SB}^3} \quad (2)$$

where $F_{y,SB}$ and K_{SB} = lateral yield strength and elastic stiffness of a pair of supporting braces, respectively; l_{SB} and A_{SB} = length and section area of one supporting brace; L = frame span; $\sigma_{y,SB}$ = tensile yield stress of steel material. These geometric and structural parameters are also interpreted in Fig. 7.

(c) *Hysteretic model and analytical modeling of SPD devices*

The analytical model of a bridge pier with the SPD device is shown in Fig. 5, referred to as SPD model later. In nonlinear dynamic time-history analysis, the SPD is modeled by three spring elements. Two horizontal spring elements and one vertical spring element are working separately in horizontal and vertical directions, as is depicted by the roll connections shown in Fig. 5. Of them, two horizontal spring elements simulate the shear resistance and deformation of a shear panel under lateral force. The resulting force-deformation response of two spring elements should be identical to the bilinear hysteretic curve on the right-hand side of Fig. 5. Chen et al.[7] proposed a set of formulas to determine the model parameters. The proposed model is simple yet accurate for predicting dissipated energy. In reality, shear panel will be inevitably subjected to vertical axial force whereas horizontal spring elements can only describe the force-displacement behavior under shear. Therefore, an additional vertical spring element is used to provide the axial stiffness of the entire shear panel. The vertical spring is assumed elastic; its stiffness is $Eb_w t_w / a$. Preliminary analyses show that the vertical spring element reduces deflections of the girder at the midpoint whereas it has almost no effect on the lateral displacement of the entire structure. The supporting braces are modeled by two-dimensional Euler-Bernoulli beam elements.

(d) *Design procedures and commentaries for SPD devices in seismic design*

In this study, a SPD device is designed to have the same values of α_F and α_K as the BRB. After basic properties of the main structure such as $F_{y,f}$ and K_f are obtained, the lateral yield resistance of SPD device, $F_{y,d}$, and its lateral stiffness, K_d, can then be easily obtained by multiplying α_F and α_K by the known $F_{y,f}$ and K_f, respectively. Once its strength and stiffness are established, the SPD device can be designed.

The next step requires a selection of the SPD depth, *a*, which is generally 1/10~1/3 times story height for building structures[13]. For bridge structures, the depth is relatively large in order to meet shear deformation demand of SPD caused by severe earthquakes. Having established the outline dimensions of SPD and $F_{y,d}$, the thickness of the web plate for SPD can be determined from Eq. (1a) with the design condition $F_{y,d} = F_{y,SPD}$. Note that the web thickness should be designed with caution to ensure the web slenderness parameter within the suggested range of 0.2 to 0.5, which can be achieved by calibrating the number of longitudinal and transverse stiffeners without change of yield shear strength. The shear stiffness of SPD, K_{SPD}, can be determined by Eq. (1a) at the same time.

Note that the lateral stiffness of an energy-dissipation device is related to the lateral stiffness of the entire SPD device composed of a SPD and two supporting braces, given by

$$\frac{1}{K_d} = \frac{1}{K_{SPD}} + \frac{1}{K_{SB}} \tag{3}$$

Since K_d and K_{SPD} are already known at this stage, K_{SB} can be obtained from Eq. (3) and subsequently $F_{y,SB}$ and A_{SB} from Eq. (2).

The strength capacity, $F_{y,SB}$, needs to be checked. Theoretically, lateral yield strength of the supporting braces is required to be slightly larger than designed shear force transferred from the SPD. In the work of Tena-Colunga and Vergara[14], the supporting braces are designed as axial steel members with a safety factor of 1.7 to prevent brace buckling. In this study, capacity of supporting braces is verified according to the JRA code[15]. The slenderness ratio of supporting braces should be less than the limit value of 150 as a secondary compression member to prevent global buckling. The designed stress in a brace is also verified by allowable stress that is specified in the JRA code[15] as a compression plate to prevent local buckling of the plate.

3.2 Buckling-restrained brace (BRB)

(a) *Basic properties of buckling-restrained braces*

To date, many types of BRB sections are used. Of them, a kind of BRB with a flat core plate developed by Nagoya University[8), 16] is used in this study. The cross section of such a BRB is shown in Fig. 6. Similar to other BRBs, its axial deformation is allowed only at the core plate, where severe buckling is eliminated by the exterior restraining members. The axial yield strength of BRB, $P_{y,BRB}$, is given by

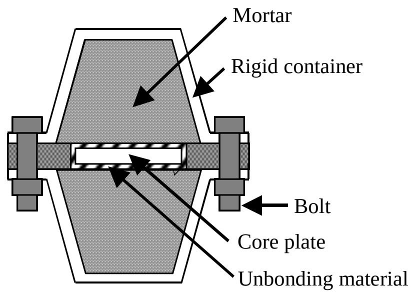

Fig.6 Cross section of BRB

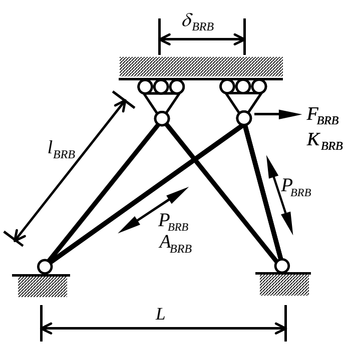

Fig.7 Schematic diagram for BRB deformation

$$P_{y,BRB} = \sigma_{y,BRB} A_{BRB} \quad (4)$$

where $\sigma_{y,BRB}$ = tensile yield stress of steel material and A_{BRB} = section area of the core plate.

The geometric parameters and basic properties of BRB are illustrated in Fig. 7. The relationship between these parameters can be expressed as follows,

$$F_{y,BRB} = K_{BRB} \cdot \delta_{y,BRB}\,,\ \ \delta_{y,BRB} = \sigma_{y,BRB} \cdot \frac{2l_{BRB}^2}{EL}\,,$$

$$K_{BRB} = A_{BRB} \cdot \frac{EL^2}{2l_{BRB}^3} \quad (5)$$

where $F_{y,BRB}$, $\delta_{y,BRB}$, and K_{BRB} = lateral yield strength, displacement, and elastic stiffness of a pair of BRBs, respectively, and l_{BRB} = length of BRB.

(b) *Hysteretic model and analytical modeling of BRB*

The analytical model of a bridge pier with BRB is shown in Fig. 8, referred to as BRB model later. BRB is directly modeled by the truss element, only carrying axial tension and compression without local bucking. In this study, the core plates of the BRB employed in Fig. 6 are made of SS400 steel. For such BRB, the bilinear stress-strain relationship with kinematic hardening rule as illustrated on the right-hand side of Fig. 8 is employed[8].

(c) *Design procedures and commentaries for BRB in seismic design*

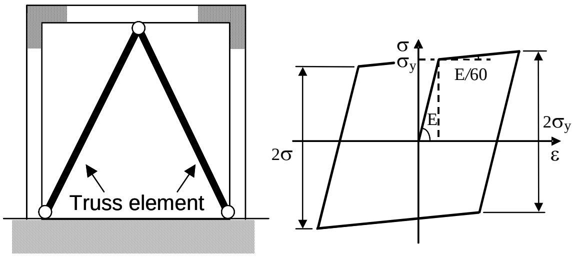

Fig.8 BRB model

As mentioned before, α_F, α_K, and α_δ are mutually dependent for this kind of BRB. That is to say, if the configuration (i.e., l_{BRB} and L) and steel material ($\sigma_{y,BRB}$) are predetermined, A_{BRB} is the sole adjustable parameter in design of BRB members. In this study, α_F is taken as 0.5, 1.0, and 1.5 to verify whether it can be used as unified design criteria. With the selected α_F, $F_{y,BRB}$ can be determined by multiplying α_F by the known $F_{y,f}$. After steel material of BRB is chosen, K_{BRB}, and A_{BRB} can easily be calculated by Eq. (5).

4. Design and Analytical Modeling of Steel Bridge Structures

4.1 Design and analytical modeling of single-deck bridge piers

The analytical model to be investigated here is single-deck steel bridge piers of frame type, which are widely used in Japan to support elevated expressways. The general layout and analytical model are illustrated in Fig. 9(a). The bridge pier is

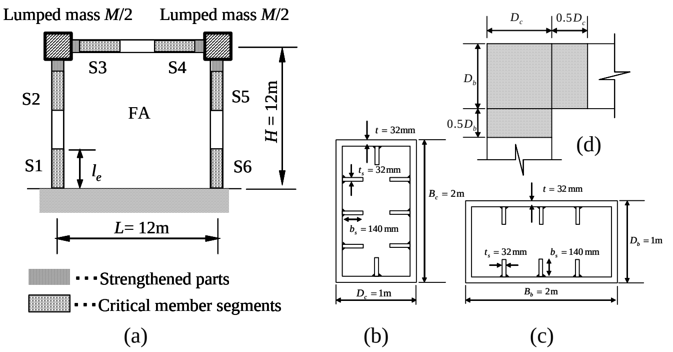

Fig.9 Single-deck steel bridge pier: (a) layout; (b) pier section; (c) girder section; and (d) details at strengthened corners

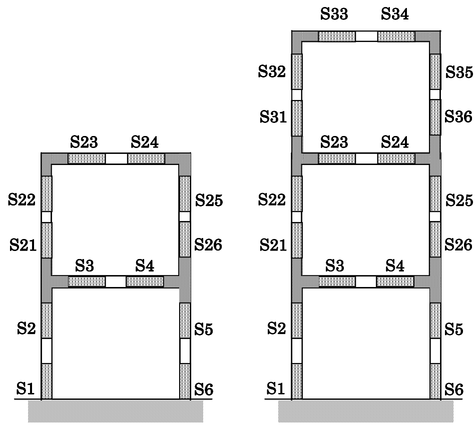

Fig.10 Multi-deck steel bridge piers

Table 1 Basic information of main structures

Model type	M ($\times 10^3$kg)	$\delta^{in}_{y,f}$ (m)	$V^{in}_{y,f}$ (kN)	$\delta_{u,f}$ (m)	$V_{u,f}$ (kN)	T_f (sec)
FA	2042	0.078	6758	0.418	11836	0.97
F2	2034	0.137	5939	0.518	10884	1.23
F3	2895	0.178	5129	0.549	9557	1.77

designed in accordance with the Seismic Coefficient Method[15), 17)], assuming Regional Class A and Ground Type II. Table 1 presents the basic properties of the single-deck bridge pier (denoted by FA), which are determined by a pushover analysis[18)]. The piers and the girder have uniform stiffened box cross-sections as shown in Figs. 9 (b) and (c). Since this type of portal frames is commonly heavy burdened, the pier-girder connection parts should be strengthened to avoid shear failure and in this study the plate thickness of the strengthened parts shown in Fig. 9(d) has been doubled. For this bridge structural form, as mentioned in the introduction, critical local damage generally appears in the compressive flange of some critical member segments[18)], which are denoted by the dotted sections at the pier bases and adjacent to the rigid corners as shown in Fig. 9 (a). Therefore, a strain-based parameter, $\varepsilon_{a)\max}$, has been suggested by Zheng et al.[19)] to estimate local damage degree of the thin-walled bridge structures. $\varepsilon_{a)\max}$ is measured at the compressive flange over an effective failure length of a critical member segment, l_e, which is taken the smaller of 0.7 times the flange width and the distance between two adjacent diaphragms.

The two-dimensional Timoshenko beam element of type B21 provided in the ABAQUS[20)] element library is used to model the piers and the girder, accounting for shear deformation. Each pier and the girder of the main frame are divided into 20 elements: 5 elements for each critical member segment, 2 elements for strengthened parts, and remains for the other parts.

In order to trace the material cyclic behavior accurately, the modified two-surface model[21)] is employed. Rayleigh damping, which is usually utilized in dynamic analysis, consists of mass proportional damping and stiffness proportional damping. Here, mass proportional damping of 5 percent is used whereas inherent stiffness proportional damping is set as zero since it is negligible if compared to the significant equivalent viscous damping due to yielding of energy-dissipation members.

4.2 Design and analytical modeling of multi-deck bridge piers

Since a popular format of highway bridge system is of low-rise (1~3 decks) frame type, double-deck and tri-deck bridge piers of frame type are under consideration. The analytical models of the double-deck and tri-deck bridge piers are shown in Fig. 10, which are denoted by F2 and F3, respectively. It is assumed that the multi-deck piers under consideration have the same cross sections of girders and piers as the preceding single-deck pier. Thus, each deck has the same yield strength and stiffness. The basic properties are presented in Table 1. The masses are uniformly imposed on the top of each column. In this study, energy-dissipation devices are installed in all levels.

5. Investigation on Seismic Performance Upgrading Effects

5.1 Efficiency of dampers in single-deck bridge piers

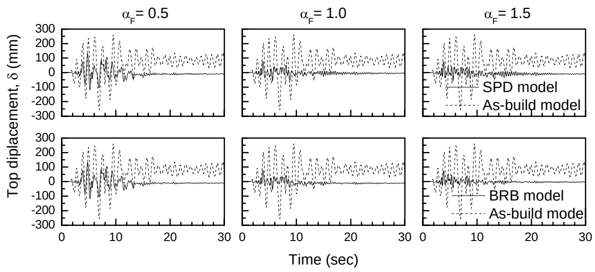

(a) Top displacement responses

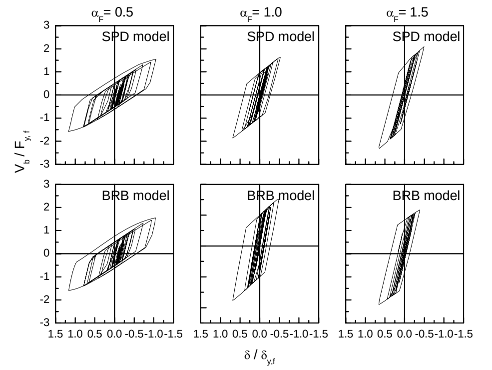

(b) Total base shear-top displacement responses

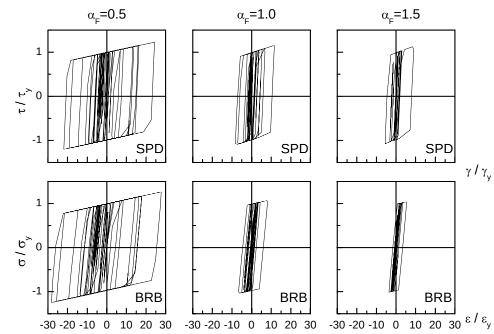

(c) Stress-strain responses of energy-dissipation members

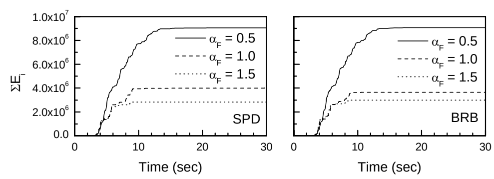

(d) Energy dissipated by energy-dissipation members

Fig.11 Comparison between SPD model and BRB model with the strength ratio α_F

(a) *Effects of the strength ratio*, α_F

In order to investigate seismic upgrading effects of energy-dissipation members, time-history analyses are conducted on single-deck bridge piers subjected to JRT-EW-M ground motion, which was recorded from the 1995 Hyogoken-Nanbu earthquake. The parameter investigated here is the strength ratio, α_F. The resulted time history responses are illustrated in Fig. 11, and maximum seismic responses are summarized in Table 2.

Shown in Fig. 11(a) are the time history responses of top displacement for the SPD model and the BRB model along with the as-build model (a pier without energy-dissipation members). It is clear that top displacement demands are greatly reduced in both the SPD and BRB models compared to the as-build model, indicating merits of installation of damping devices. Shown in Fig. 11(b) are the time-history responses of total base shear versus top displacement of SPD and BRB models. With the same α_F, the curves of the SPD model and the BRB model are almost alike in the shape, showing similar global seismic performances. It can be seen that the model of α_F = 0.5 shows somehow isotropic behavior in the largest loops, compared with those of the models of α_F = 1.0 and 1.5. This is because that a plastic zone develops in the main structure, which is modeled by the modified two-surface model rather than the simplified bilinear model. Such plastic zones can be verified by the large value of $\varepsilon_{a)\max}/\varepsilon_y$ = 3.3 or 3.5, as presented in Table 2, which is measured at Part S6 for FA-SPD(BRB)-05. The stress-strain responses of SPD and BRB members are shown in Fig. 11(c). Larger deformation is observed in SPD than in BRB in the cases of α_F = 1.0 and 1.5, but it is reverse in the case of α_F = 0.5. In contrast to the different deformation demands in SPD and BRB, energies dissipated by two types of energy-dissipation members are in a good agreement as shown in Fig. 11(d). It implies that SPD suffers severer damage than BRB although energy dissipation capacity is similar. The difference in local deformation results from the configuration of energy-dissipation devices in the piers because the web length of SPD is a quarter of the pier height while the BRB length is almost half of the diagonal. In Fig. 11(d), it can also be found that SPD and BRB yield simultaneously and continue dissipating input energy until the pulse of ground motion vanishes. Overall, their stable energy dissipating capacity is confirmed in all cases.

Table 2 presents normalized maximum responses obtained from time-history analyses. Compared with the responses of the as-build model, the major reduction of performance responses, i.e., $\varepsilon_{a)\max}/\varepsilon_y$, $\delta_{\max}/\delta_{y,f}$, $\gamma_{\max}/\gamma_y)_{SPD}$, and $\varepsilon_{\max}/\varepsilon_y)_{BRB}$ has verified the substantial improvement of seismic performances for structures installed with energy-dissipation members. The maximum average compression strain, $\varepsilon_{a)\max}$, of the as-build model is 23.4ε_y at the base of the pier (in this case at critical member segment denoted by S6), with a sharp decrease of about 3.0ε_y (moderate damage) in the case of α_F = 0.5, 1.0ε_y (light damage) in the case of α_F = 1.0, and 0.9ε_y (no damage) in the case of α_F = 1.5. The maximum top displacement, $\delta_{\max}$, is decreased from 2.3δ_y (moderate damage) to below 1.7δ_y (light damage). For the total base shear, adding dampers does not result in significant increase of total base shear compared to that of as-build model, which benefits the retrofit of foundations because foundation strengthening will require major labor efforts.

A further comparison of efficiency of BRB and SPD devices reveals that seismic demands of both energy-dissipation members are almost similar in terms of global performances,

Table 2 Comparison between SPD model and BRB model with the strength ratio α_F

Model	$\dfrac{\varepsilon_{a)\max}}{\varepsilon_y}$	$\dfrac{\delta_{\max}}{\delta_{y,f}}$	$\dfrac{V_{b,\max}}{F_{y,f}}$	$\left.\dfrac{\gamma_{\max}}{\gamma_y}\right)_{SPD}$	$\left.\dfrac{\varepsilon_{\max}}{\varepsilon_y}\right)_{BRB}$
FA- As-build	23.4	2.32	1.19	–	–
FA-SPD-05	3.3	1.17	1.58	24.4	–
FA-BRB-05	3.5	1.17	1.59	-	28.2
FA-SPD-10	1.0	0.69	1.86	11.6	–
FA-BRB-10	1.0	0.69	1.77	–	8.2
FA-SPD-15	0.9	0.66	2.31	9.0	–
FA-BRB-15	0.9	0.66	2.20	–	5.4
FB-SPD-10	1.3	0.81	2.11	23.6	–
FB-BRB-10	0.9	0.68	1.77	–	8.0
FC-SPD-10	0.9	0.63	1.81	11.8	–
FC-BRB-10	1.0	0.66	1.75	–	7.8

Note: FA, FB, and FC represent three shape-type frames, respectively. BRB and SPD represent frame with BRB and SPD devices, respectively. The numbers of 05, 10, and 15 represent the α_F values of 0.5, 1.0, and 1.5.

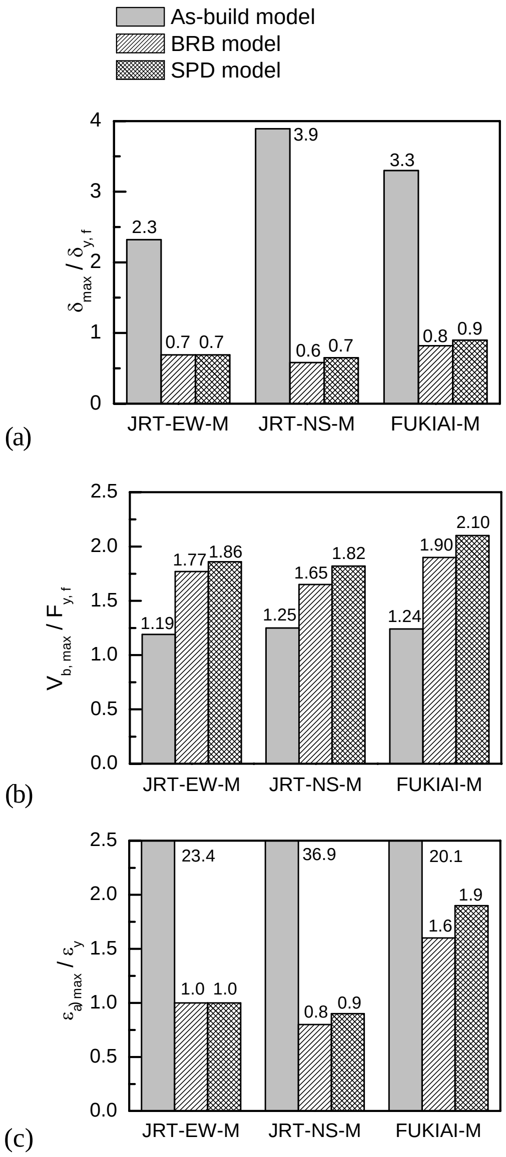

Fig.12 Comparison under various strong earthquakes

Table 3 Comparison between SPD model and BRB model with the strength ratio α_F

Model	$\frac{\varepsilon_{a)\max}}{\varepsilon_y}$	$\delta_{\max}$ (m)	$V_{b,\max}$ ($\times 10^3$kN)	$\left.\frac{\varepsilon_{\max}}{\varepsilon_y}\right)_{BRB}$	$\left.\frac{\gamma_{\max}}{\gamma_y}\right)_{SPD}$	$\frac{E_f}{E_p}$	$\frac{E_{d,1}}{E_p}$	$\frac{E_{d,2}}{E_p}$	$\frac{E_{d,3}}{E_p}$	E_p ($\times 10^6$J)
F2- As-build	27.8	0.531	11.1	–	–	1.000	–	–	–	26.7
F2-BRB-03	1.11	0.154	16.3	5.2	–	0.001	0.470	0.529	–	8.59
F2-SPD-03	1.00	0.156	16.7	–	10.5	0.000	0.427	0.573	–	8.74
F2-BRB-05	1.65	0.169	23.1	4.6	–	0.006	0.255	0.739	–	6.67
F2-SPD-05	1.36	0.169	23.8	–	11.4	0.003	0.233	0.765	–	6.85
F3-As-build	21.5	0.699	10.7	–	–	1.000	–	–	–	18.7
F3-BRB-03	1.38	0.289	19.4	9.4	–	0.002	0.193	0.484	0.321	11.6
F3-SPD-03	0.93	0.283	20.1	–	19.2	0.000	0.198	0.446	0.356	11.1

Note: F2 and F3 stand for double-deck and tri-deck bridge piers, respectively. As-build represents BRB and SPD represent BRB and SPD devices, respectively. The numbers of 03 and 05 represent the α_F values of 0.3 and 0.5 at each level. E_p represents the total plastic energy; E_f and $E_{d,i}$ represent plastic energy in the main frame and in the dampers of each level, respectively, where i = 1, 2, and 3.

such as $\delta_{\max}$, $V_{b,\max}$, and $\varepsilon_{a)\max}$. It is indicated that if the structures are designed based on α_F, α_K, and α_δ, their behavior is alike no matter which energy-dissipation member is employed. However, the damage degree to the members is different. In the case of α_F = 0.5, the normalized shear deformation of SPD, $\gamma_{\max}/\gamma_y)_{\mathrm{SPD}}$, and the normalized axial deformation of BRB, $\varepsilon_{\max}/\varepsilon_y)_{\mathrm{BRB}}$, are 24.4 and 28.2, respectively. In reality, fracture failure may occur in steel plates if it is over the limit value of 20[22]. Thus, the values of 24.4 and 28.2 are considered only for qualitative analysis. As α_F is increased from 0.5 to 1.0, a rapid decrease of deformation of energy-dissipation member is observed, indicating damage mitigation to the main structure. Meanwhile, increasing α_F from 1.0 to 1.5, the maximum responses are slightly improved. When α_F equals 1.5, the main structure remains elasitc. This fact indicates that the main structure can remain intact even under a strong earthquake.

(b) *Effects of frame shape*

To further understand the seismic behavior of energy-dissipation members in bridges with different shape, time-history analyses are performed on additional two bridge piers subjected to the JRT-EW-M ground motion. The original pier of square shape is denoted by FA. FB denotes a pier with H = 18m and L = 12m, and FC denotes a pier with H = 12m and L = 18m. Their natural periods are correspondingly changed to 1.46 sec for FB pier and 1.0 sec for FC pier, respectively. The strength ratio α_F is taken as 1.0. The resulting seismic responses are summarized in Table 2. As can be seen, the maximum response results of FA and FC match greatly well. A good agreement of the performance parameters and damper's deformation can also be seen between two cases because of the close natural period. In the case of FB-SPD-10, average compression strain and top displacement demands are found to be larger than those in the cases of FA-SPD-10 and FC-SPD-10. It is because that the stiffness of FB-SPD-10 is smaller than the other two structures. Large seismic responses result in large shear deformation of 23.6 in the SPD, which exceeds the limit value of 20. It is obvious that the energy-dissipation capacity of the designed SPD is not enough for such kind of frame shape.

(c) *Effects of various strong ground motions*

To further investigate the efficiency of energy-dissipation members under various strong ground motions, total of three strong ground motions, which are recorded from the 1995 Hyogoken-Nanbu Earthquake, are used in this study. They are commonly used for limit-state verification purposes[17].

The comparison results are shown in Fig. 12. Clearly, the top displacement demands of SPD and BRB models sharply decrease compared to those of as-build model (see Fig. 12(a)). In Fig. 12(b) the total base shear resulting from the added stiffness is no more than twice of the original one. As a result, foundation retrofit is not required. Fig. 12(c) shows a good agreement of average compressive strain between SPD and BRB models. All these observations are consistent with previous findings.

5.2 Efficiency of dampers in multi-deck bridge piers

Dynamic analysis results of multi-deck bridge piers are summarized in Table 3. As can be seen from the table, BRB and SPD models with the same α_F yield good agreements on the global performance responses such as top displacement demand and total base shear demand. Major findings obtained from single-deck bridge piers can be extended to multi-deck ones. In contrast, implementation of energy-dissipation members in multi-deck bridge piers has a particular problem about distribution of damping devices into the story. In Table 3, it is found that plastic energy dissipates averagely at each level in the case of F2-BRB-03, in which $E_{d,1}/E_p$ is equal to 0.470 and $E_{d,2}/E_p$ is equal to 0.529. In the case of F2-SPD-03, they are 0.427 and 0.573, respectively. The excellent energy distribution results from a suitable distribution of stiffness and strength of damping devices in the two cases. However, highly unequal energy distribution exists for both cases of F2-BRB-05 and F2-SPD-05. For the BRB model, the damper in the first level dissipated 0.225 of the total plastic energy while 0.739 in the second level. For the SPD model, they are 0.236 and 0.763. Non-uniform distribution of dissipated energy causes the ineffective reduction of structural responses. Although the strength ratio increases from 0.3 to 0.5, F2-05 series produce large strains and top displacements than F2-03 series do. Non-uniform distribution of dissipated energy can be found in F3 series as well. The optimum distribution of damping devices into bridge structures will be one of the important issues in the future research.

6. Design and Fabrication Considerations

From design viewpoint, predictions of seismic performances for structures with hysteretic dampers can be easily achieved by controlling the yield strength ratio and the stiffness ratio. For SPD, the practical design according to the target performance can be established by adjusting the geometry and steel material of dampers. However, restrained by the predefined condition, namely, requirement of a larger yield strength of supporting frames than that of SPD, the cross section of supporting braces is prone to be large and cause the rigidity of damping device significantly high. On the other hand, for BRB, once its steel material and geometric size are established, so do the yield strength and yield deformation of BRB devices. The fixed relationship between yield strength and deformation allows less flexibility in the design of BRB devices.

From economical viewpoint, utilization of hysteretic damping devices can largely reduce construction cost if compared to the seismic retrofit method, for example, to stiffen cross sections or add stiffeners to reduce the width-to-thickness ratio of plate components. As has been indicated from the obtained statistic of the seismic retrofit cost of a large span truss bridge[23], the implementation of BRB can reduce 50 percent cost compared to the conventional retrofit measures.

For BRB and SPD concerned here, the construction costs include costs of dampers and surrounding equipments, labor force, installation cost etc. SPD can be manufactured simply and directly from steel plates. The construction cost of SPD depends mostly on the cutting, welding, assembling costs of steel plates, and non-corrosive paint. BRB members are commercially available, whose prices depend on manufacturers. As a result, there is no reliable information to quantitatively compare the cost of SPD and BRB. Nevertheless, the cost relates largely to the weight of consumed steel material.

In the aspects of installation and replacement, both BRB and SPD devices are of maintenance-free. They are also convenient to be replaced due to bolt connection. Furthermore, since SPD can be divided into several small panels, as introduced in the preceding subsection, it also shows favorable transport and erection performance. Additionally, the settlement of supporting braces into main structure is almost the same as that of a common H-section brace, and can be built easily also at the time of a main structural erection. After severe earthquakes, replacement of SPD is also easy. Since supporting braces are designed to remain in the elastic range, only the steel shear panel part needs to be replaced. Hence, operation platform can be set only at the upper position, saving space and keeping passageway unblocked.

7. Conclusions

In this paper, detail design and analytical modeling technologies were provided for steel bridge structures with two types of energy-dissipation members: shear panel dampers (SPD) and buckling-restrained braces (BRB). An extensive numerical study was conducted on different steel bridge piers of frame type installed with such members. Main findings from this study are concluded as follows:

(1) Both BRB and SPD are effective on dissipating earthquake-induced energy and eliminating or limiting damage to the main structures
(2) If designed with the same strength ratio, stiffness ratio or other equivalent parameters, the controlled structures would generate almost similar global seismic demands regardless of the selected energy-dissipation member type;
(3) Local deformation of SPD will be larger than that of BRB due to their geometric configuration in the structures;
(4) The performance-based verification method, making use of displacement and strain indices, proves to be applicable in thin-walled steel framed bridges installed with energy-dissipation members;
(5) For civil engineers, choosing SPD or BRB depends on all aspects of design, construction, and maintenance.

Acknowledgements: The financial support from National Research Institute for Earth Science and Disaster Prevention (NIED) through the Bridge Seismic Experiment Research Project of International Cooperation Research Projects using the 3-D Full-scale Earthquake Testing Facility (E-Defense) is greatly appreciated.

References

1) Bergman, D. M. and Geol, S. C., Evaluation of cyclic testing of steel-plate devices for added damping and stiffness, *Rep. No. UMCE 87–10*, Univ. of Michigan, Ann Arbor, Mich., 1987.
2) Tsai, K. C., Chen, H. W., Hong, C. P. and Su, Y. F., Design of steel triangular plate energy absorbers for seismic-resistant construction, *Earthquake Spectra* 9(3), pp.505-528, 1993.
3) Nakashima, M., Iwai, S., Iwata, M., Takeuchi, T., Konomi, S., Akazawa, T. and Saburi, K., Energy dissipation behaviour of shear panels made of low yield steel, *Earthq. Eng. Struct. Dyn.* 23(12), pp.1299-1313, 1994.
4) Zahrai, S. M. and Bruneau, M., Ductile end-diaphragms for the seismic retrofit of slab-on-girder steel bridges, *J. Struct. Eng.*, ASCE 125(1), pp.71-80, 1999.

5) Usami, T., Lu, Z. H. and Ge, H. B., A seismic upgrading method for steel arch bridges using buckling-restrained braces, *Earthq. Eng. Struct. Dyn.* 34, pp.471-496, 2005.
6) Zheng, Y., Usami, T. and Ge, H. B., Ductility evaluation procedure for thin-walled steel structures, *J. Struct. Eng.*, ASCE 126(11), pp.1312-1319, 2000.
7) Chen, Z. Y., Ge, H. B. and Usami, T., Hysteretic model of stiffened shear panel dampers, *J. Struct. Eng.*, ASCE 132(3), pp.478-483, 2006.
8) Watanabe, N., Kato, M., Usami, T. and Kasai, A., Experimental study on cyclic elasto-plastic behavior of buckling-restrained braces, *Journal of Earthquake Engineering*, JSCE 27, pp.1-8, 2003. (in Japanese)
9) Inoue, K. and Kuwahara, S., Optimum strength ratio of hysteretic damper, *Earthq. Eng. Struct. Dyn.* 27, pp.577-588, 1998.
10)Ye, L. P. and Ouyang, Y. F., Dual seismic structure system and its parametric analysis, *Engineering Mechanics* 17 (2), pp.23-29, 2000 (in Chinese).
11)Yamaguchi, H. and Ashraf, E. A., Effect of earthquake energy input characteristics on hysteretic damper efficiency, *Earthq. Eng. Struct. Dyn.* 32, pp.827-843, 2003.
12)Nakashima, M., Saburi, K. and Tsuji, B., Energy input and dissipation behaviour of structures with hysteretic dampers, *Earthq. Eng. Struct. Dyn.* 25, pp.483-496, 1996.
13)JSSC, Seismic response behaviour and design method for frame structures with hysteretic dampers, *Japanese Society of Steel Construction*, Tokyo, Japan, 1998 (in Japanese).
14)Tena-Colunga, A. and Vergara, A., Comparative study on the seismic retrofit of a mid-rise steel building: steel bracing vs energy dissipation, *Earthq. Eng. Struct. Dyn.* 26, pp.637-655, 1997.
15)JRA, Design Specifications of Highway Bridges-Part II Steel Bridges, *Japan Road Association*, Tokyo, Japan, 2002 (in Japanese).
16)Kato, M., Usami, T., and Kasai, A., An experimental study on cyclic elasto-plastic behavior of buckling restrained brace members, *Proceedings of the 6th Symposium on Ductility Design Method for Bridges*, Ductility Design Subcommittee, Earthquake Engineering Committee, JSCE, Tokyo, Japan, pp. 345-350, 2003 (in Japanese).
17)JRA, Design Specifications of Highway Bridges-Part V Seismic Design, *Japan Road Association*, Tokyo, Japan, 2002 (in Japanese).
18)Usami, T., Zheng, Y. and Ge, H. B., Seismic design method for thin-walled steel frame structures, *J. Struct. Eng.*, ASCE 127, pp.137-144, 2001.
19)Zheng Y., Usami, T. and Ge, H. B., Ductility of thin-walled steel box stub-columns, *J. Struct. Eng.*, ASCE 126(11), pp.1304-1311, 2000.
20)ABAQUS, Inc. ABAQUS/Analysis user's manual–version 6.4. Pawtucket, R.I., 2003.
21)Shen, C., Mamaghani, I. H. P., Mizuno, E. and Usami, T., Cyclic behavior of structural steels. II: theory, *Journal of Engineering Mechanics*, ASCE 121(11), 1165–1172, 1995.
22)Kasai, A., Watanabe, T., Amano, M. and Usami, T., Strength and ductility evaluation of stiffened steel plates subjected to cyclic shear loading, *J. Struct. Eng.*, JSCE 47A, pp.761-770, 2001 (in Japanese).
23)Kanaji, H., Takada, Y. and Mino, T., Study on cost reduction of a long span truss bridge retrofitted with hysteretic dampers, Proc. of Japan Road Conference, Vol.25, 2003.

(Received: September 11, 2006)